

# Suprabasin enhances the invasion, migration, and angiogenic ability of oral squamous cell carcinoma cells under hypoxic conditions

ASAMI HOURI, YOSHIKI MUKUDAI, YUZO ABE, MASATAKA WATANABE, MAKI NARA, SAYA MIYAMOTO, MAI KURIHARA, TOSHIKAZU SHIMANE and TATSUO SHIROTA

Department of Oral and Maxillofacial Surgery, School of Dentistry, Showa University, Ota-ku, Tokyo 145-8515, Japan

Received September 14, 2022; Accepted January 9, 2023

DOI: 10.3892/or.2023.8520

**Abstract.** Suprabasin (SBSN) is a secreted protein that is isolated as a novel gene expressed in differentiated keratinocytes in mice and humans. It induces various cellular processes such as proliferation, invasion, metastasis, migration, angiogenesis, apoptosis, therapy and immune resistance. The role of SBSN was investigated in oral squamous cell carcinoma (OSCC) under hypoxic conditions using the SAS, HSC-3, and HSC-4 cell lines. Hypoxia induced SBSN mRNA and protein expression in OSCC cells and normal human epidermal keratinocytes (NHEKs), and this was most prominent in SAS cells. The function of SBSN in SAS cells was analyzed using 3-(4,5-dimethylthiazol-2-yl)-2,5-diphenyltetrazolium bromide (MTT); 5-bromo-2'-deoxyuridine (BrdU); cell cycle, caspase 3/7, invasion, migration, and tube formation assays; and gelatin zymography. Overexpression of SBSN decreased MTT activity, but the results of BrdU and cell cycle assays indicated upregulation of cell proliferation. Western blot analysis for cyclin-related proteins indicated involvement of cyclin pathways. However, SBSN did not strongly suppress apoptosis and autophagy, as revealed by caspase 3/7 assay and western blotting for p62 and LC3. Additionally, SBSN increased cell invasion more under hypoxia than under normoxia, and this resulted from increased cell migration, not from matrix metalloprotease activity or epithelial-mesenchymal transition. Furthermore, SBSN induced angiogenesis more strongly under hypoxia than under normoxia. Analysis using reverse transcription-quantitative PCR showed that vascular endothelial growth factor (VEGF) mRNA was not altered by the knockdown or overexpression of SBSN VEGF, suggesting that VEGF is not located downstream of SBSN. These results

demonstrated the importance of SBSN in the maintenance of survival and proliferation, invasion and angiogenesis of OSCC cells under hypoxia.

## Introduction

Oral squamous cell carcinoma (OSCC), which includes cancers of the head and neck, is a highly malignant disease with high morbidity and mortality rates worldwide (1). Of the patients diagnosed with OSCC, 50% exhibit lymph node metastases, which is correlated with poor prognosis; the OSCC survival rates have not changed during the last 30 years (2). The disease frequently occurs on the tongue, upper and lower gingiva, palate, oral floor, and buccal mucosa. Previously, Sasahira and Kirita (3) reviewed prognostic factors for OSCC and described the '10 hallmarks of cancer', (sustained proliferative signaling, evasion of growth suppressors, circumvention of immune destruction, activation of invasion and metastasis, tumor-promoting inflammation, enabling of replicative immortality, induction of angiogenesis, genome instability and mutation, resistance to cell death, and dysregulation of energetics). However, treatment to curtail the progression of cancer has not yet been established, despite an increase in related research.

Oxygen is essential for energy metabolism in the body, but rapid tumor growth affects the surrounding vascular system, which results in reduced oxygen levels and the creation of hypoxic regions (4). The tumor microenvironment is composed of various cellular and non-cellular components, including the normal and immune cells surrounding the tumor tissue. Most tumors cause hypoxia due to increased oxygen consumption and inadequate supply (5). Persistent hypoxia increases the irregular distribution of tumor vasculature and the distance from capillaries (4). Tumor cells adapt to hypoxia and have an important effect on various cells and their physiological functions. The increased expression of hypoxia-inducible factor 1 $\alpha$  (HIF-1 $\alpha$ ) is an important marker of hypoxia around tumor cells (4-7); HIF has a central role in the cellular mechanism that responds to hypoxia. HIF-1 $\alpha$  activation is involved in cellular infiltration, metastases, metabolic reprogramming and resistance to therapy (7-10). To adapt to hypoxia, tumor cells develop into blood vessels. Therefore, an important

---

*Correspondence to:* Dr Yoshiki Mukudai, Department of Oral and Maxillofacial Surgery, School of Dentistry, Showa University, 2-1-1 Kitasenzoku, Ota-ku, Tokyo 145-8515, Japan  
E-mail: mukudai@dent.showa-u.ac.jp

**Key words:** suprabasin, squamous cell carcinoma, oral cancers, cell proliferation, cell invasion, angiogenesis, hypoxia

feature of the hypoxic response is angiogenesis. Angiogenesis and lymph-angiogenesis are required for the growth, invasion and metastasis of tumor cells (3). Metastasis is the main cause of cancer-related death (6). Hypoxia and HIF are involved in several different steps of metastasis and induce tumor cell invasion and degradation of the extracellular matrix (ECM) (6).

Suprabasin (SBSN) is a secreted protein that has been isolated as a novel gene expressed in differentiated keratinocytes in mice and humans. It has been detected in the basal layers of the epithelia of the tongue, esophagus, stomach, epidermis, and lung, as well as in invasive glioblastoma cells (11-14). The SBSN isoform is presumed to be a signaling molecule, similar to AKT (15) and WNT/ $\beta$ -catenin (16), and it induces cellular proliferation, invasion, metastasis, migration, angiogenesis, apoptosis, therapy (15-17) and immune resistance. Shao *et al* (17) revealed that SBSN is important for maintaining the ability of invasion and metastasis and anchorage-independent growth in salivary gland adenoid cystic carcinoma (ACC). In addition, SBSN expression was shown to be upregulated by the demethylation of CpG islands, and SBSN was found to be significantly hypomethylated in primary ACC compared with that in normal salivary gland tissue (17). Furthermore, it has been reported that overexpression of SBSN in esophageal squamous cell carcinoma (ESCC) increases proliferation and tumorigenicity and induces migration and angiogenesis in human tumor endothelial cells (TEC) isolated from two carcinomas, renal and colon, and the AKT pathway is a downstream factor of SBSN (15,16,18). Liu *et al* (19) reported that SBSN mRNA levels increased in OSCC treated with inactive *Prophyromonas gingivalis*. Besides, SBSN has been reported to be involved in the development and progression of cancer and has a role in treatment resistance (20). Therefore, SBSN may serve as a promising biomarker for these cancers. However, there are few studies that show the relationship between SBSN and cancer under hypoxic conditions, where tumor cells are known to respond differently during adaptation. Thus, it was hypothesized that SBSN would affect tumor cells under hypoxic conditions and its role in OSCC under such conditions was investigated. The present results revealed that SBSN is important in cell proliferation, cell migration and vascular induction into OSCC cells under hypoxia.

## Materials and methods

**Cell culture.** Human OSCC-derived cell lines, SAS (21,22), HSC-3 (22,23) and HSC-4 (22,23), were cultured in high-glucose Dulbecco's modified Eagle's medium (HDMEM) with L-glutamine and phenol red (FUJIFILM Wako Pure Chemical Corporation) supplemented with 10% fetal bovine serum (FBS), 100 U/ml penicillin, and 100 mg/ml streptomycin at 37°C, with 5% CO<sub>2</sub> and 100% humidity. Normal human epidermal keratinocytes (NHEKs) were purchased from PromoCell GmbH and cultured in endothelial cell growth medium (PromoCell GmbH), according to the manufacturer's protocol. Human umbilical vein endothelial cells (HUVEC) were purchased from Lonza Group, Ltd. and cultured in an EGM-2 Endothelial Cell Growth Medium-2 BulletKit (CC-3162) (Lonza Group, Ltd.) according to the

manufacturer's protocol. Hypoxic conditions were set at 37°C, 2% O<sub>2</sub>, and 5% CO<sub>2</sub> in a BIOLABO mini-multi-gas incubator (BL-43MD; TOSC Japan Ltd.).

**Antibodies.** Rabbit monoclonal anti-HIF1- $\alpha$  (cat. no. ab179483) and anti-HIF-2 $\alpha$  (cat. no. ab199) and polyclonal anti-SBSN (cat. no. ab232771) antibodies were purchased from Abcam. Rabbit polyclonal anti-E-cadherin (cat. no. 20874-1-AP), anti-N-cadherin (cat. no. 22018-1-AP) and anti- $\beta$ -actin (cat. no. 20536-1-AP) antibodies were purchased from Proteintech Group, Inc. Rabbit monoclonal anti-LC3A/B (D3U4C; cat. no. 12741) and anti-SQSTM1/p62 (D1Q5S; cat. no. 39749) were purchased from Cell Signaling Technology, Inc. Rabbit polyclonal anti-HaloTag antibody (cat. no. G9281) was purchased from Promega Corporation. Mouse monoclonal anti-endocrine gland-derived vascular endothelial growth factor (EG-VEGF) antibody was purchased from Santa Cruz Biotechnology, Inc. (E-12; cat. no. sc-390741). The anti-rabbit IgG and horseradish peroxidase-linked whole secondary antibody (from donkey) was purchased from Merck Millipore (cat. no. NA934V). Otherwise, primary and secondary antibodies for cyclin proteins were used from the Cyclin Antibody Sampler Kit (cat. no. 9869; Cell Signaling Technology, Inc.).

**RNA purification and reverse transcriptase polymerase chain reaction (RT-qPCR).** Total cellular RNA was purified using TRIzol<sup>®</sup> reagent (Thermo Fisher Scientific, Inc.) according to the manufacturer's protocol and stored at -80°C until use. Total cellular RNA (100 ng) was reverse-transcribed using the ReverTra Ace qPCR RT Kit (Toyobo Life Science) according to the manufacturer's protocol. The generated cDNA was subjected to RT-qPCR using the THUNDERBIRD Probe qPCR Mix (Toyobo Life Science) according to the manufacturer's protocol. Final concentrations of the primers were 20  $\mu$ l each. The PCR cycles were 95°C for 1 min, 95°C for 15 sec, 60°C for 30 sec (for 49 cycles). TaqMan primers were purchased from Thermo Fisher Scientific, Inc. (SBSN, cat. no. Hs01078781; VEGF, cat. no. Hs00900055; and  $\beta$ -actin, cat. no. Hs01060665). After qPCR, statistical analysis was performed using the CFX Connect Real-Time PCR Detection System (Bio-Rad Laboratories, Inc.). Gene expression was analyzed using the 2<sup>- $\Delta\Delta C_q$</sup>  method (24) and normalized to that of  $\beta$ -actin.

**Protein preparation and western blot analysis.** Total cellular protein was prepared as previously described (21). For western blot analysis, 20  $\mu$ g of total cellular protein was analyzed using sodium dodecyl sulfate-polyacrylamide gel electrophoresis (SDS-PAGE) with a 4-20% gradient gel (Bio-Rad Laboratories, Inc.) and blotted onto a polyvinylidene difluoride membrane with iBlot2 (Thermo Fisher Scientific, Inc.). After transcription, the membrane was shaken for 1 h in Tris-buffered saline (Takara Bio, Inc.) containing 0.2% non-fat dry milk (Cell Signaling Technology, Inc.). Primary and secondary antibody reactions were performed as previously described (25). Protein bands were visualized using Amersham ECL Prime Western Blotting Detection Reagent (Cytiva) and a ChemiDoc XRS Plus Image Lab System (Bio-Rad Laboratories, Inc.), which was also used to measure the density of each band.

**Gene transfection.** Small interfering RNA (siRNA) for human SBSN (EHU016151) and negative control siRNA (for firefly luciferase, EHUFILUC) were purchased from Sigma-Aldrich; Merck KGaA. The expression vectors HaloTag-SBSN (pFN21AE2798) and HaloTag control vector (G659) were purchased from Promega Corporation. The siRNAs and expression vectors were transfected into the cells using Lipofectamine 2000 Transfection Reagent (Thermo Fisher Scientific, Inc.) according to the manufacturer's protocol and a recent study (22).

**3-(4,5-dimethylthiazol-2-yl)-2,5-diphenyltetrazolium bromide (MTT), caspase 3/7, and 5-bromo-2'-deoxyuridine (BrdU) assays.** Cells were seeded in six-well tissue culture plates at a density of  $6 \times 10^5$  cells/well for MTT and caspase 3/7 assays and in 48-well tissue culture plates at a density of  $1.2 \times 10^5$  cells/well for the BrdU assay. After incubation under normoxic conditions for 24 h, the cells were transfected with siRNAs or expression vectors as aforementioned. The day after transfection, the cells were reseeded in 96-well tissue culture plates at a density of  $5 \times 10^2$  cells/well for MTT and apoptotic assays and in 96-well tissue culture plates at  $5 \times 10^2$  cells/well for the BrdU assay. The cells were exposed to normoxic or hypoxic conditions. After 0, 1, and 3 days, MTT and caspase 3/7 assays were performed, as previously described (21). The BrdU assay was performed after 3 days using a commercially available kit (CytoSelect BrdU Cell Proliferation ELISA Kit; Cell Biolabs Inc.).

**Crystal violet cell staining.** Transfected cells were reseeded in 96-well tissue culture plates as aforementioned. The cells were exposed to normoxic or hypoxic conditions, and after 1 and 3 days, they were fixed with 4% paraformaldehyde phosphate buffer solution (FUJIFILM Wako Pure Chemical Corporation) at 4°C for 30 min and stained with 0.5% crystal violet (FUJIFILM Wako Pure Chemical Corporation) in 20% methanol at room temperature for 5 min. Images were captured using an BX51 microscope (Olympus Corporation) and a microscopic CCD camera (Olympus DP71), and microscopic images were analyzed using commercial software (Olympus cellSens standard).

**Cell cycle assay.** Cell seeding and transfection were performed as in the MTT and caspase 3/7 assays. The day after transfection, the cells were reseeded in six-well tissue culture plates at a density of  $6 \times 10^5$  cells/well and exposed to either normoxic or hypoxic conditions for 3 days. The cell cycle assay was performed by using a commercially available kit (Tali Cell Cycle Kit; cat. no. A10798; Thermo Fisher Scientific, Inc.) according to the manufacturer's protocol and a recent study (26), and they were analyzed using a Tali Image-Based Cytometer (Thermo Fisher Scientific, Inc.).

**Cell invasion assay.** Cell invasion assay was performed using a commercially available kit (CytoSelect 24-Well Cell Invasion Assay; Cell Biolabs Inc.). After transfection, the medium was replaced with fresh medium and the cells were exposed to either normoxic or hypoxic conditions for another 48 h. A 1-ml aliquot of condition medium from each well was collected and centrifuged at  $10,000 \times g$  for 3 min at 4°C, and the supernatant was stored on ice before use.

Next,  $1.0 \times 10^6$  SAS cells were suspended in serum-free high glucose DMEM, and the cell suspension was placed in the upper chamber (polycarbonate membrane inserts with 8- $\mu$ m pores, with an upper surface coated with a uniform layer of dried basement membrane matrix solution). The chamber was incubated with 500  $\mu$ l of conditioned medium (as aforementioned) in a 24-well plate for 48 h under normoxic or hypoxic conditions at 37°C. After the removal of non-invasive cells from the basement membrane, invasive cells were stained and quantified according to the manufacturer's protocol. Images were captured, as aforementioned.

**Wound healing assay.** This assay was performed according to previous studies (21,25,27), with slight modifications. The transfected cells were reseeded in a 24-well tissue culture plate at a density of  $2.4 \times 10^5$  cells/well, were exposed to normoxic conditions for 24 h. Scratches were made using 1-ml pipette chips, and the wells were washed twice with phosphate-buffered saline (PBS). The cells were allowed to proliferate for another 24 h under normoxic or hypoxic conditions. Then, the cells were fixed at 4°C for 30 min and stained at room temperature for 30 min with 0.5% crystal violet in 20% methanol, and images were captured, as aforementioned.

**Gelatin zymography.** This assay was performed using a commercially available kit (Gelatin-zymography kit, Code No. AK47; Cosmo Bio Co., Ltd.). After a 24-h incubation post transfection, the medium was replaced with fresh medium. The cells were exposed to normoxic or hypoxic conditions for 48 h. The conditioned medium (500  $\mu$ l) was collected, centrifuged  $10,000 \times g$  at 4°C for 3 min, and concentrated to 20  $\mu$ l by Amicon Ultra-0.5 10k centrifugal filter unit (Merck Millipore). Next, 10  $\mu$ l of concentrated aliquot was subjected to gelatin zymography according to the manufacturer's protocol.

**Tube formation assay.** The tube formation assay was performed using a commercially available kit (Endothelial Tube Formation assay; Cell Biolabs Inc.) according to the manufacturer's protocol, as previously described (15). The SAS cells were seeded into 24-well tissue culture plates at a density of  $1.0 \times 10^5$  cells/well and transfected as aforementioned. After 24 h, the medium was changed to EGM-2 and the cells were incubated for an additional 48 h under normoxia. A 1-ml aliquot of conditioned medium was collected, centrifuged at  $10,000 \times g$  for 3 min, and stored on ice until needed. Next,  $2.0 \times 10^5$  HUVEC cells were suspended in each conditioned medium and overlaid onto an ECM gel set in a 96-well plate, according to the manufacturer's protocol. The cells were incubated for 24 h under normoxic or hypoxic conditions, examined, and images were captured using a phase-contrast microscope system (Nikon Eclipse TS-100 and DS-R1i; Nikon Corporation).

**Mice.** The present study complied with the ARRIVE guidelines and the AVMA euthanasia guidelines 2020, was approved (approval nos. 14033 and 14034) by the Institutional Animal Care and Use Committee of Showa University (Tokyo, Japan) and conducted in accordance with the Showa University Guidelines for Animal Experiments. Four-week-old female BALB/cAJcl-nu/nu mice (~20 g) were purchased from Claire

Japan (Tokyo) and maintained under pathogen-free conditions as previously described (21). Each group included three mice (nine mice per an experiment) and thereby, thirty-six mice in total were used. SAS, HSC-3 and HSC-4 cells ( $\sim 1.0 \times 10^6$ ) in 100  $\mu$ l saline were injected subcutaneously into a unilateral flank, and the cancer-bearing mice were maintained for 40 days to develop tumors, according to a previous study by the authors (22). Movement disorders, anorexia, nausea, and abnormal behavior were to be expected due to cancer growth and metastasis, causing distress and stress to the mice. If the mice exhibited body weight loss of more than 10% in 7 days, abnormal behavior by excessive stress such as self-injury or other injury or damage to the breeding gauge, or if the size of the primary tumor exceeded 4 cm<sup>3</sup>, the experiment was to be terminated immediately by CO<sub>2</sub> asphyxiation, even before the set end point (day 40). However, in the present study, since no mice showed these abnormal behaviors, all mice were sacrificed at 40 days without interrupting the experiment. At the end point, the mice were sacrificed by CO<sub>2</sub> asphyxiation. After confirmation of death by palpation, the tumor was resected, as described in our previous study (22). The day when the cells were injected into the mice was set as day 0. Tumor volumes were measured every 20 days. Tumor volume was determined by direct measurement and calculated using the formula:  $\pi/6 \times (\text{large diameter}) \times (\text{small diameter})^2$  (22).

**Histology.** Resected specimens were fixed with 10% formalin at 4°C for 2 days, embedded in paraffin, and stained with hematoxylin and eosin (H&E Stain Kit; Sakura Finetek) for 5 min each as previously described (21,22).

**Statistical analysis.** All experiments were performed at least four times, and data was presented as the mean  $\pm$  standard deviation. Statistical analyses were performed using the Tukey's test as post hoc for two-way analysis of variance (ANOVA). Statistically significant difference was determined at  $P < 0.05$ . All analyses were carried out using the KaleidaGraph version 4.5 software (Hulinks, Inc.) as previously described (22,28).

## Results

**Hypoxia increases SBSN expression.** Previous studies have shown that SBSN is highly expressed in tumor cells and affects several cancer cells (13-17). OSCC cells were transplanted into the right unilateral flanks of mice (Fig. S1A). The transplanted SAS cells showed the highest ability to form tumors (Fig. S1B and C). The tumor formed by the HSC-4 cells was too small to be histopathologically sectioned. Since H&E staining (Fig. S1D) showed differences in cell differentiation between the SAS and HSC-3 cells, an *in vitro* study was conducted to further investigate whether hypoxia induced the expression of SBSN genes and proteins in the OSCC and NHEK cells (Fig. 1). The SBSN mRNA was upregulated in each cell type under hypoxic conditions ( $P < 0.05$ ). In OSCC cells (SAS, HSC-3 and HSC-4), SBSN mRNA was strongly increased by hypoxia in a time-dependent manner, but this effect was weaker in the NHEK cells (Fig. 1A). Western blot analysis (Fig. 1B and C) revealed similar results as observed in RT-qPCR, although expression of cellular SBSN was faint. In addition, VEGF, which is located at the downstream of

HIF, a marker of hypoxia, was increased under hypoxia conditions, which was in consistency with previous studies (29,30). However, the signal strength of VEGF in OSCC was weak, and in NHEK it was barely detected. These results indicated that SBSN is more crucial in OSCC cells under hypoxia than in NHEK cells. Notably, since SBSN mRNA and protein levels were highest in SAS cells, these cells were used as representatives of OSCC cells in the following experiments.

**SBSN increases cell proliferation and decreases apoptosis and autophagy.** The effects of SBSN on cell proliferation under hypoxia were investigated using the MTT (Fig. 2A), BrdU (Fig. 2B), and cell cycle (Fig. 2C and D) assays. Knockdown of SBSN increased MTT activity ( $P < 0.05$ ) and overexpression of SBSN decreased MTT activity ( $P < 0.05$ ). However, in the BrdU assay, which directly examined actively proliferating cells, SBSN knockdown decreased BrdU incorporation ( $P < 0.05$ ). Additionally, overexpression of SBSN increased under normoxic and hypoxic conditions ( $P < 0.05$ ), and this increase was more pronounced under hypoxia. In addition, the cell cycle assay showed similar results to the BrdU assay. Western blotting for cyclin-related proteins (Fig. S2A) indicated involvement of the cyclin pathways. Crystal violet cell staining (Fig. S2B) showed that the cells under all conditions were under exponential proliferating phase and that even on day 3, they did not reach confluency, indicating little consideration for contact inhibition. These results indicated that SBSN increased cell proliferation under normoxia and hypoxia. To investigate this discrepancy between the assays, the effects of SBSN on representative cell death, apoptosis and autophagy were examined by using a caspase 3/7 assay (Fig. 3A) and western blotting for p62 and LC3 (Fig. 3B). Knockdown of SBSN decreased caspase 3/7 activity ( $P < 0.05$ ); however, SBSN overexpression had little decreasing effect ( $P < 0.05$ ) under normoxia. Both SBSN knockdown and overexpression had a slightly increasing effect ( $P < 0.05$ ) on caspase 3/7 activity under hypoxia, which was weaker than that under normoxia. In addition, SBSN knockdown increased both the degradation of p62 and the conversion of LC3-I to LC3-II, and overexpression of SBSN showed the opposite effect under normoxia. Similar results were obtained under hypoxic conditions. These results indicated that although the effects were weak, SBSN suppresses autophagy in SAS cells, regardless of the oxygen partial pressure. Western blotting also showed the successful transfection of siRNAs and expression vectors.

**SBSN increases cell invasion and migration.** The effects of SBSN on cell invasion were investigated using a cell invasion assay (Fig. 4A and B). Knockdown of SBSN decreased cell invasion, and SBSN overexpression increased it under normoxia or hypoxia ( $P < 0.05$ ). Notably, the increase in cell invasion was more prominent under hypoxic conditions than under normoxic conditions. As this effect was considered to be due to increased cell migration (15), ECM protein degradation (31-33), and promotion of epithelial-mesenchymal transition (EMT) (32,34-36), the effect of SBSN on cell migration, matrix metalloprotease (MMP) activity, and EMT was investigated using wound healing assay (Fig. 4C and D), gelatin zymography (Fig. 4E), and western blotting for E-cadherin

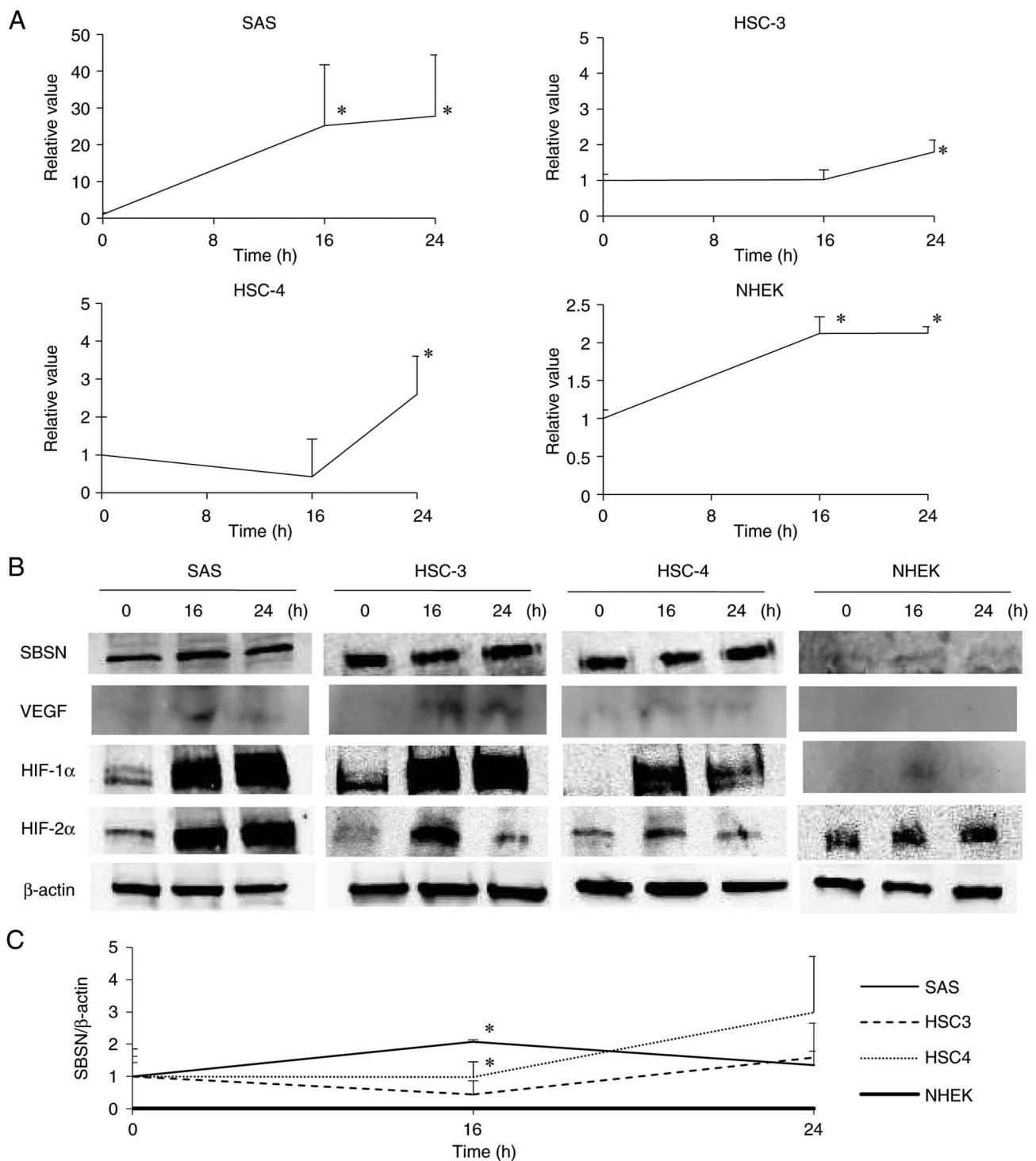


Figure 1. Induction of SBSN in OSCC and NHEK cells under hypoxia. SAS, HSC-3, HSC-4 and NHEK cells were exposed to hypoxia for 0, 16 and 24 h. (A) The SBSN mRNA levels in SAS, HSC-3, HSC-4 and NHEK cells were analyzed using reverse transcription-quantitative PCR. (B) The SBSN, VEGF, HIF-1α, HIF-2α and β-actin protein levels were analyzed using western blotting and band densities divided by that of β-actin of each band in four individual experiments are shown with standard deviations (C). The value at time 0 is designated as '1', and relative values are shown. \*P<0.05 vs. time 0. All experiments were performed four times at least, and a representative result is shown. SBSN, suprabasin; OSCC, oral squamous cell carcinoma; HIF, hypoxia-inducible factor.

and N-cadherin (Fig. 4F), respectively. The cell migration assay (Fig. 4C and D) revealed that SBSN knockdown suppressed cell migration and that overexpression of SBSN promoted migration under both normoxic and hypoxic conditions (P<0.05). The increasing effect of SBSN was stronger under hypoxia than under normoxia, as observed in the cell invasion assay. However, gelatin zymography (Fig. 4E) showed

that knockdown or overexpression of SBSN had no significant or little effect on the alteration of secreted MMP activity (ProMMP-9, ProMMP-2, and MMP-2), regardless of normoxia or hypoxia. Furthermore, western blotting for E-cadherin and N-cadherin, which are representative EMT markers (Fig. 4F), was performed. E-cadherin expression was increased by both SBSN knockdown and SBSN overexpression. However, the

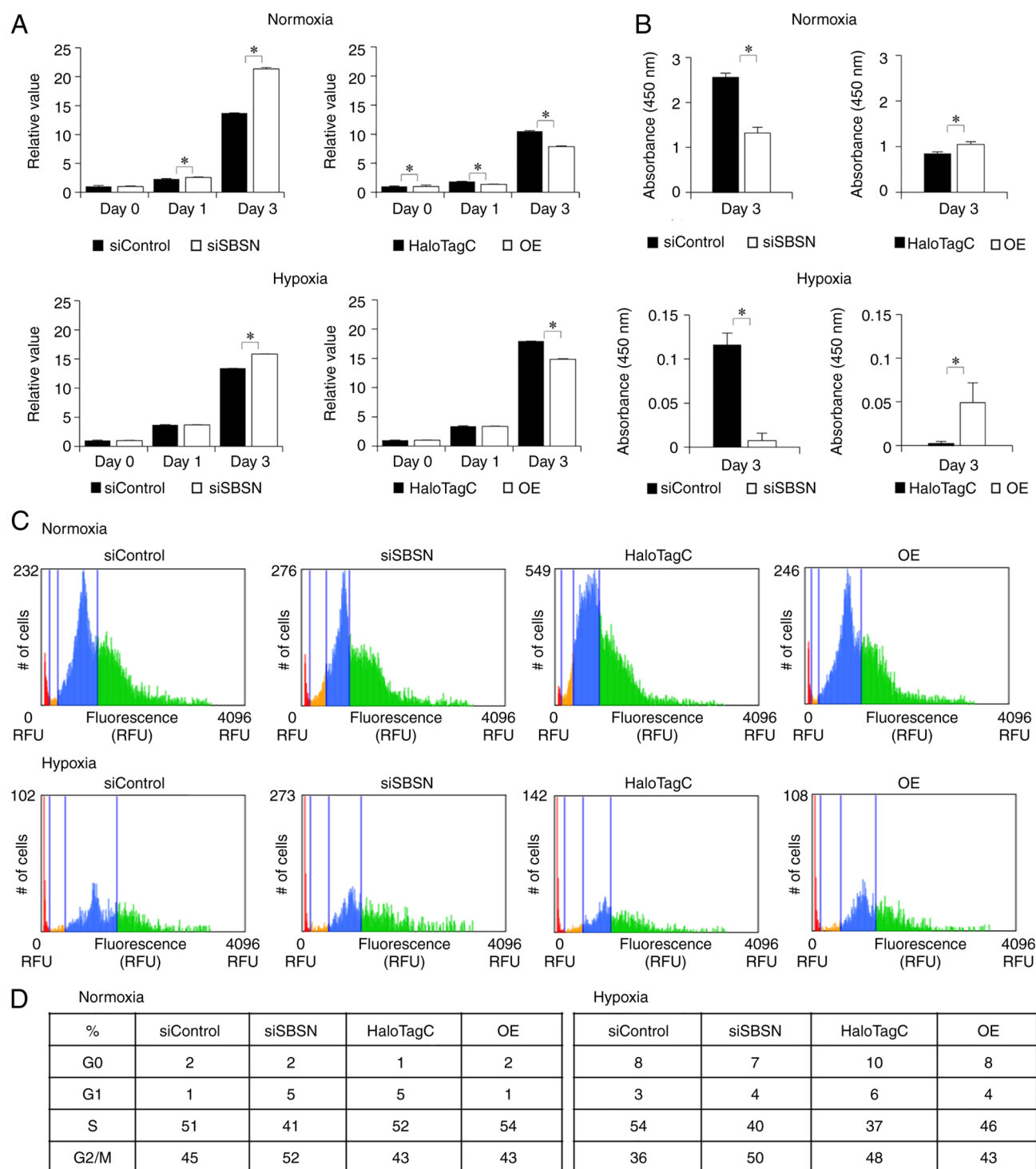


Figure 2. Effects of knockdown and overexpression of SBSN on growth of SAS cells. In this experiment, siRNA for SBSN or control siRNA, and HaloTag-SBSN (OE) or HaloTag control vector, were transfected into SAS cells and incubated under normoxic conditions for 24 h. Next, the cells were exposed to normoxic or hypoxic conditions. After 0, 1 and 3 days, cells were subjected to the (A) MTT assay and (B) BrdU assay, and the (C and D) cell cycle assay. For the MTT assay, the value at day 0 is designated as '1', and relative values are shown. The value of results was subjected to ANOVA. \* $P < 0.05$  vs. control. In panel D, the percentage of cell-cycle phase (G0 and G1, S, and G2/M) in each sample is shown in a table. All experiments were performed four times at least, and a representative result is shown. SBSN, suprabasin; siRNA, small interfering RNA; OE, overexpression; BrdU, 5-bromo-2'-deoxyuridine; OE, overexpression.

expression of N-cadherin was increased by SBSN knockdown and decreased by SBSN overexpression. These effects were similar under both normoxia and hypoxia. Importantly, these results showed that SBSN knockdown or overexpression had no significant involvement in EMT. According to these results, SBSN increased cell invasion while MMP activity and

EMT did not, and these effects resulted from increased cell migration.

*SBSN induces angiogenic ability of OSCC cells.* As a previous study has reported that SBSN affects tube formation in tumor endothelial cells (15), the relationship between SBSN

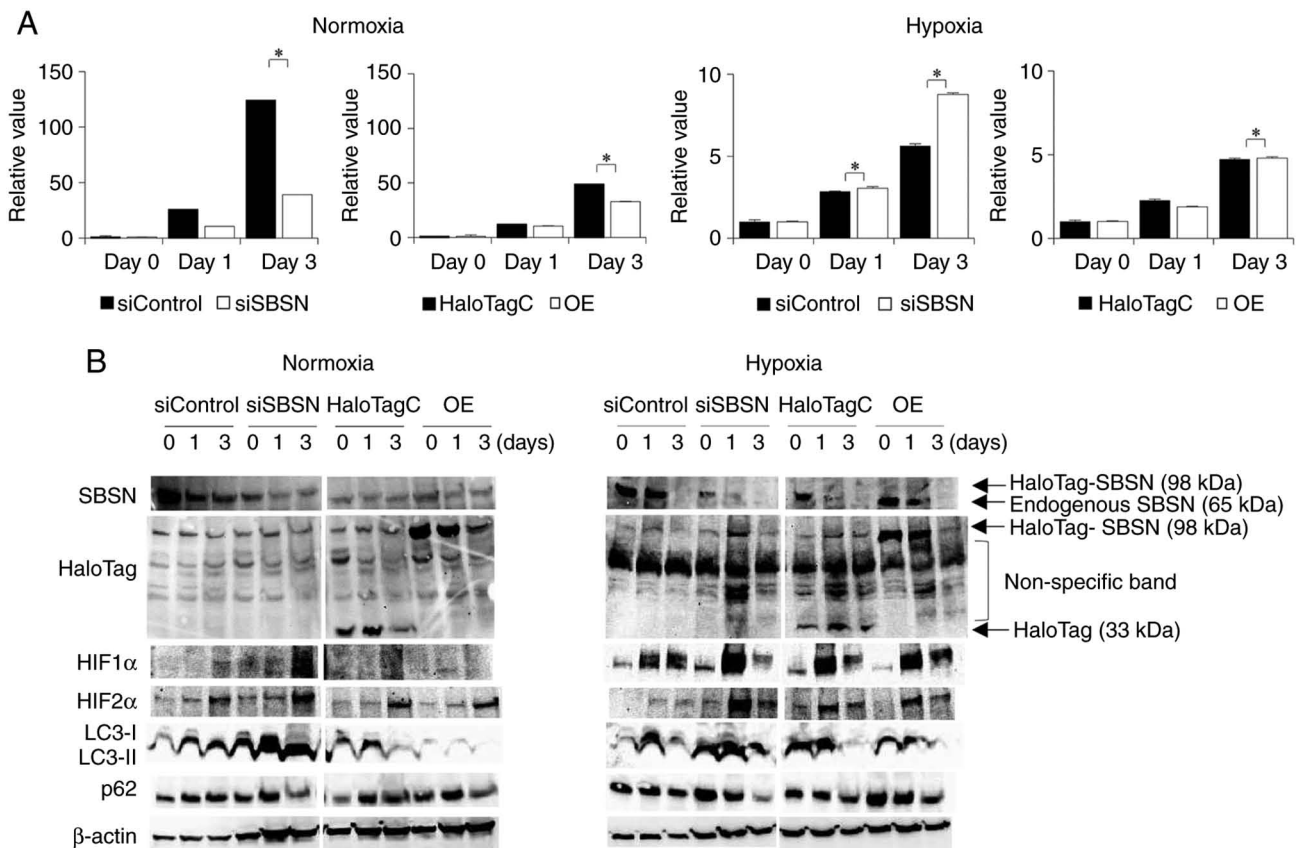


Figure 3. Effects of knockdown and overexpression of SBSN on apoptosis and autophagy of SAS cells. (A) First, siRNA for SBSN or control siRNA, and HaloTag-SBSN (OE) or HaloTag control vector, were transfected into SAS cells and incubated under normoxic conditions for 24 h. Next, the cells were exposed to normoxic or hypoxic conditions. After 0, 1 and 3 days, either (A) the cells were subjected to caspase 3/7 assays or (B) total cellular proteins were subjected to western blot analysis to detect SBSN and HaloTag (overexpressed and endogenous proteins are indicated by arrows along with each molecular weight on the right side of right panel), as well as HIF-1 $\alpha$ , HIF-2 $\alpha$ , LC3-I, LC3-II, p62 and  $\beta$ -actin. For caspase 3/7 assays, the value at day 0 is designated as '1', and relative values are shown. The value of results was subjected to ANOVA. \* $P < 0.05$  vs. control. All experiments were performed four times at least, and a representative result is shown. SBSN, suprabasin; siRNA, small interfering RNA; OE, overexpression; HIF, hypoxia-inducible factor.

and angiogenesis was investigated using a tube formation assay (Fig. 5). In this assay, angiogenic ability of SBSN in SAS cells was assessed by counting the number of junctions formed in endothelial tubes. Overexpression of SBSN under normoxia and hypoxia induced angiogenesis. Knockdown of SBSN suppressed this effect while overexpression increased this effect. These effects were more prominent under hypoxic conditions than under normoxia. This result indicated that SBSN induced angiogenesis. It has been reported that expression of HIF-1 $\alpha$  is upregulated, which activates transcription of pro-angiogenic factors such as VEGF (37). Finally, the relationship between SBSN and VEGF under hypoxia was investigated (Fig. S3). Knockdown of SBSN slightly increased, and SBSN overexpression slightly decreased, VEGF mRNA ( $P < 0.05$ ). These results indicated that VEGF gene expression is not located downstream of SBSN.

## Discussion

The center of a tumor is subjected to hypoxia, and several studies have shown that hypoxia-induced HIF-1 $\alpha$  expression (38,39) is involved in the malignant progression of OSCC. Tumor cells have been shown to promote adaptation to hypoxia and contribute to cell invasion, cell survival and

angiogenesis (6,7,39,40). Accordingly, resistance to treatment and the prognosis of patients have been revealed to be related to tumor hypoxia (6-10). Pribyl *et al* (41) reviewed the general functions of SBSN, and Tan *et al* (42) also reviewed the specific roles of SBSN in cancer and other diseases. However, the role of SBSN under hypoxic conditions in OSCC cells has not yet been reported. Therefore, in the present study, focus was addressed on the role of SBSN under hypoxia and SAS, HSC-3 and HSC-4 cells was used as representative OSCC cells. It was demonstrated that SAS cells formed the largest tumor in the tumor xenograft experiment. In previous studies, SBSN was found to have a poor prognosis in ESCC, and it was considered that the secretion of SBSN may be positively correlated with the malignancy of the cancer. The SAS cells are known to have the highest malignancy in OSCC, and in preliminary experiments, the different tumor sizes were identified to affect the malignancy of the cancer. It was hypothesized that the secretion of SBSN in SAS with the highest malignancy would correlate with the malignancy of the cancer and the expression of SBSN in different cell lines. The present *in vitro* experiment showed that SAS cells expressed the highest levels of SBSN. These results are consistent with a previous study revealing that the expression of SBSN mRNA was upregulated in ESCC cells (16). Therefore, it was hypothesized that SBSN is involved



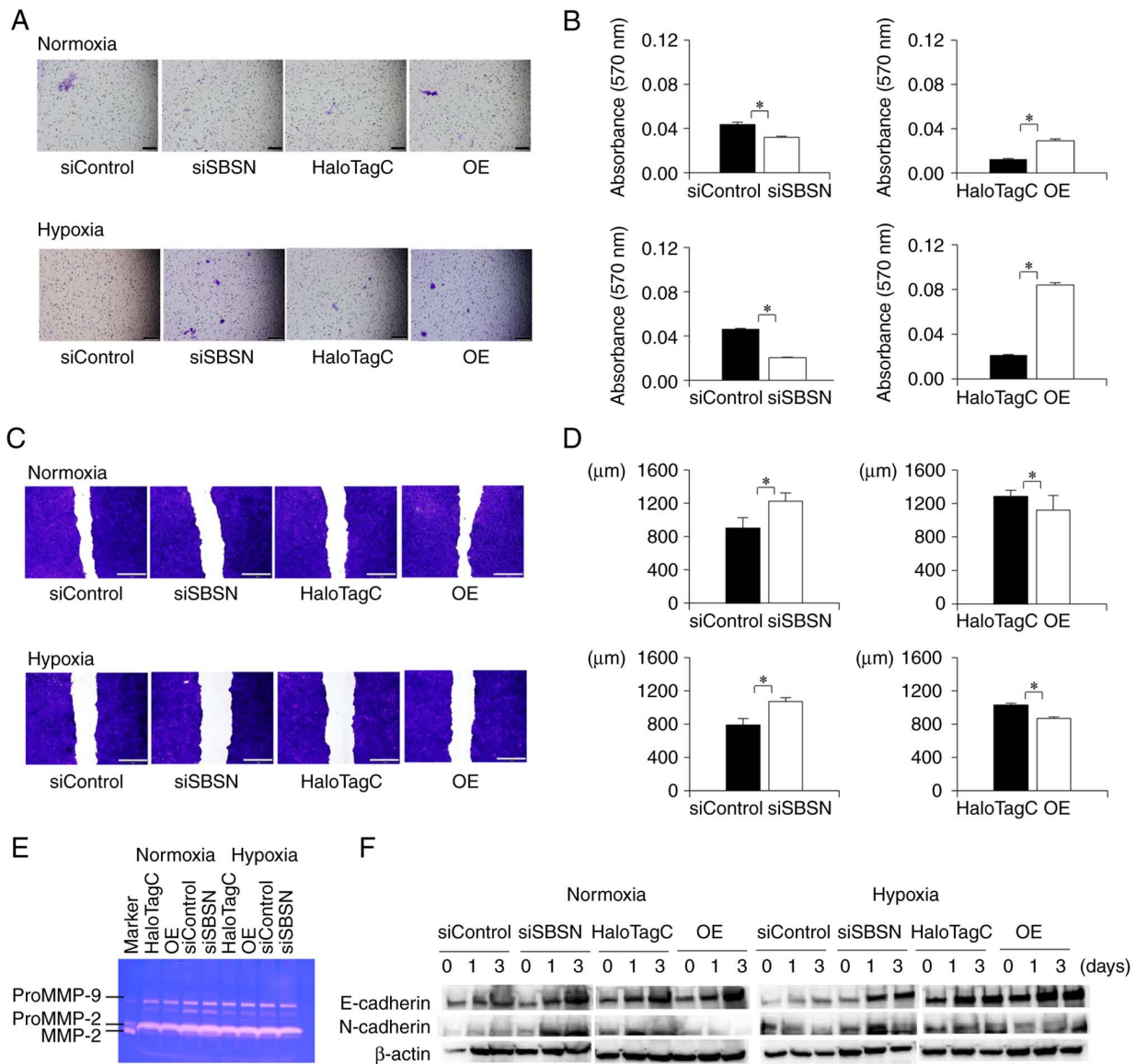


Figure 4. Effects of knockdown and overexpression of SBSN on cell invasion, migration, MMP activities, and EMT. First, siRNA for SBSN or control siRNA, and HaloTag-SBSN (OE) or HaloTag control vector, were transfected into SAS cells. (A and B) Cell invasion assay in which the transfected cells were incubated under normoxic or hypoxic conditions for 48 h. From these, 1-ml aliquots of the condition medium were collected and used as chemoattractants. Freshly suspended SAS cells were subjected to cell invasion assay for 48 h. Then, the invasive cells were stained by crystal violet. (A) Images of the invasive cells were captured and (B) the optical absorbance of destained solution from the membrane was measured. (C and D) Wound healing assay. The transfected cells were reseeded to a 24-well tissue culture plate, exposed to normoxic or hypoxic conditions for 24 h, and subjected to a cell migration assay. (E) Gelatin zymography, in which the transfected cells were exposed to normoxic or hypoxic conditions for 48 h, the condition medium was collected and concentrated, and 10-ml aliquots of each concentrated condition medium were subjected to gelatin-zymography. (F) Western blotting analysis for epithelial-mesenchymal transition, in which the transfected cells were exposed to normoxic or hypoxic conditions for 0, 1 and 3 days. Next, total cellular proteins were subjected to western blot analysis to detect E-cadherin, N-cadherin and  $\beta$ -actin. The values in panels (B) and (D) were subjected to ANOVA. \* $P < 0.05$  vs. control. Scale bars: (A) 200  $\mu$ m (x100) and (C) 1 mm (x40). All experiments were performed four times at least, and a representative result is shown. SBSN, suprabasin; MMP, matrix metalloprotease; siRNA, small interfering RNA; OE, overexpression.

in the proliferation and tumorigenesis of OSCC cells under hypoxic conditions. Among OSCC, SAS is known to be one of the most malignant (22), thus it was considered that SBSN may be a prognostic biomarker in cancer cells.

Next, the relationship between SBSN and cell proliferation was investigated using the MTT, BrdU and cell cycle assays (Fig. 2). The SBSN decreased MTT activity but increased BrdU incorporation and accelerated the cell cycle under hypoxic and normoxic conditions. In addition, western blotting for cyclin-related proteins was performed and showed involvement of the cyclin pathways, although further detailed

experiments concerning relationship between cyclin pathway and cell cycle should be performed. Zhu *et al* (16) reported that MTT and BrdU assays showed that SBSN overexpression promoted the growth and proliferation of ESCC. To address the discrepancy between those assays in the present study, it was hypothesized that since the MTT assay examines cell proliferation and viability by measuring mitochondrial enzyme activity, the results of this assay may not always reflect cell proliferation alone. It was previously identified that SAS cells have high proliferation ability and high malignancy even under hypoxic conditions (21,22,25). Wigerup *et al* (6)



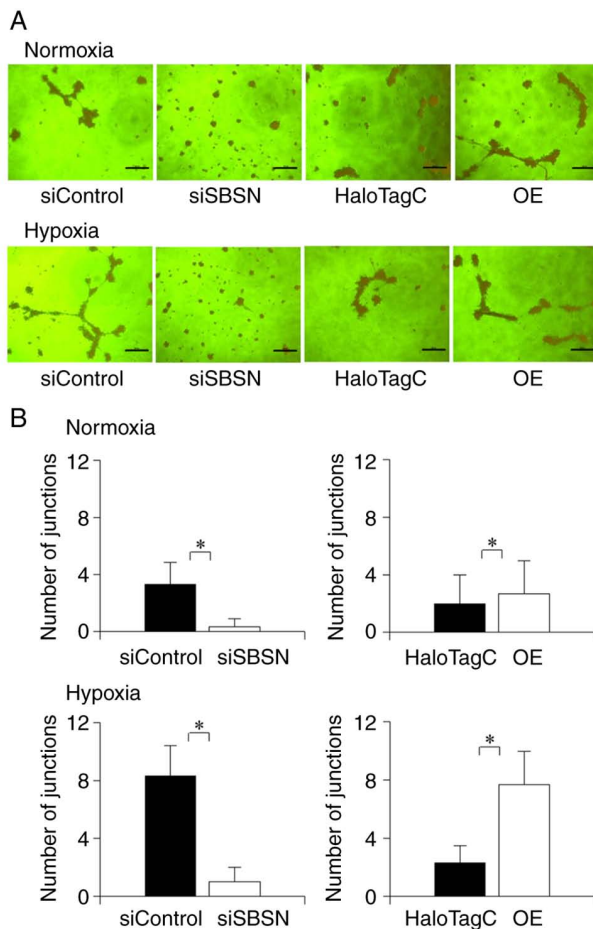


**Figure 5.** Effects of knockdown and overexpression of SBSN on *in vitro* angiogenesis. (A) First, siRNA for SBSN or control siRNA, and HaloTag-SBSN (OE) or HaloTag control vector were transfected into SAS cells and incubated under normoxic conditions for 24 h. Next, the culture medium was changed to serum-free EBM-2 medium, and the cells were cultured for another 48 h under normoxic conditions. The conditioned medium of SAS cells was collected for tube formation assay. The experimental HUVEC cells were suspended by the conditioned medium of SAS cells and were subjected to tube formation assay. After 24 h, (A) images of the cells were captured, and (B) formed junctions of the endothelial tubes were counted under a microscope. The results were subjected to ANOVA. \* $P < 0.05$ . Scale bars: 200  $\mu\text{m}$  (x200). All experiments were performed four times at least, and a representative result is shown. SBSN, suprabasin; siRNA, small interfering RNA; OE, overexpression.

demonstrated that hypoxic tumor cells attempt to survive by decreasing cell proliferation and increasing apoptosis and autophagy functions. It has been suggested that SBSN function may be involved in cell survival by increasing apoptosis under hypoxia. To address this discrepancy, more detailed experiments should be conducted. It was concluded that the results of the MTT assay may be related to SBSN secretion rather than to only cell proliferation. These results suggested that SBSN is slightly involved in cell proliferation via several signaling pathways such as the cyclin-related signal.

The autophagosome LC3 is localized to autophagosomes (28,43), while p62 is selectively integrated into autophagosomes and degraded by interactions with LC3 (28,44). Induction of autophagy converts LC3-I to LC3-II, and autophagy degrades p62. Therefore, LC3 and p62 as autophagy markers were used. Western blotting for LC3

and p62 (Fig. 3B) showed that SBSN has an inhibitory role on autophagy in SAS cells under both normoxia and hypoxia. In addition to normal and cancer cells, autophagy is known to be involved in the adaptation of normal cells to metabolic stress, such as hypoxia. This phenomenon may have suppressive and/or enhancing effects on cancer cells (*e.g.*, suppression of metastasis and limitation of necrosis and inflammatory cell infiltration in early-stage cancers and promotion of metastasis in advanced cancers) (45-49). Furthermore, it was revealed that SBSN acted in an autophagy suppressive manner. As Su *et al* (46) demonstrated that over-activated autophagy under stress conditions results in cell death, the results of the present study suggested that SBSN may suppress over-activated autophagy to protect SAS cells from excessive cell death under hypoxia.

Alam *et al* (15) reported that SBSN knockdown inhibited migration and tube formation in mouse tumor endothelial cells, thus cell invasion of SBSN under normoxic and hypoxic conditions was examined using a cell invasion assay. The results demonstrated that SBSN enhanced cell invasion, and the effects were stronger under hypoxia than under normoxia. Cell invasion has been reported to result from cell migration (32,50), degradation of ECM proteins by MMPs (3,31), and increased EMT (3,32,34,35). The effects of SBSN on cell migration, MMP activities, and EMT were also examined using wound healing assays, gelatin zymography, and western blotting for E-cadherin and N-cadherin, respectively. It was found that SBSN enhanced cell migration ability, and the effects were stronger under hypoxia than under normoxia. However, SBSN barely altered MMP activity or EMT and had repressive effects on EMT. Alam *et al* (15) reported that SBSN affects cell migration. Importantly, the present study showed that SBSN enhanced cell invasion and migration, and its effects were more prominent in hypoxia. Previous studies (3,6,7,50) have demonstrated that tumor cells induce degradation of the ECM by MMPs and increased EMT, as well as cell invasion and migration. The effects of SBSN on cell invasion and migration may be related to several other signaling pathways. To clarify this, more detailed investigations should be performed.

Based on the studies of Alam *et al* (15) and Takahashi *et al* (18), wherein SBSN expression induced cell migration and angiogenesis, the relationship between angiogenesis and SBSN under normoxic and hypoxic conditions was examined. It was identified that SBSN induced angiogenesis, which is consistent with the results of previous studies. Notably, this function is prominently enhanced under hypoxic conditions. Several previous studies (3,5,6,37,40,51) have found that tumor cells induce various transcription factors, including HIF-1 $\alpha$ , to adapt to hypoxia, resulting in induced angiogenesis (*i.e.*, formation of new blood vessels to prevent hypoxic conditions). Therefore, angiogenesis is essential for tumor cell growth, invasion and metastasis, and it is enhanced under hypoxia (51). Furthermore, Zhang *et al* (30) demonstrated that HIF-1 $\alpha$  regulates the transcriptional activation of the VEGF gene and that hypoxia increases HIF-1 $\alpha$  expression, whereby angiogenesis is promoted, followed by increased VEGF expression. Melincovici *et al* (37) also reported that hypoxia is the most important trigger for the induction of angiogenesis, and Alam *et al* (15) reported that SBSN knockdown had no significant effect on VEGF receptor mRNA

expression in mouse TEC (mTEC). Based on these results, the relationship between SBSN knockdown or overexpression under hypoxia and VEGF mRNA (Fig. S3). It was found that VEGF mRNA was slightly upregulated and downregulated by SBSN knockdown and overexpression, respectively. These results suggest that VEGF is not located downstream of SBSN. Alam *et al* (15) demonstrated that the AKT pathway is a downstream factor of SBSN, and Melincovici *et al* (37) showed that VEGF binding to VEGFR-2 leads to downstream PI3K signaling, resulting in the activation of the AKT pathway for angiogenesis as a cell survival function. Based on the results of the present study and those of previous studies, VEGF is not located downstream of SBSN, and there may be several other signaling pathways between SBSN and VEGF.

In the present study, focus was addressed on SBSN in OSCC cells under hypoxia using *in vitro* experiments and it was found that SBSN slightly affects cell proliferation and cell death. More importantly, it was revealed that SBSN was a factor in cell invasion and angiogenesis, which is in the process of investigation by the authors using *in vivo* experiments. This finding indicated the potency of SBSN as a molecular target for cancer therapy. However, the functions of SBSN under hypoxic conditions, such as the relationship between SBSN and HIF and the signaling pathways, remain to be investigated. Aoshima *et al* (52) reported that SBSN expression in the epidermis is decreased in atopic dermatitis lesional skin compared with healthy skin, and that decreased expression of SBSN suggested abnormal differentiation of epidermal keratinocytes and induction of apoptosis. Pribyl *et al* (53) reported that SBSN is expressed in the bone marrow by myeloid cell subpopulations, including myeloid-derived suppressor cells, and is secreted into bone marrow plasma and peripheral blood of myelodysplastic syndromes patients. Furthermore, the aforementioned study revealed that the highest expression of SBSN is present in a patient group with poor prognosis, and that SBSN is a candidate biomarker of high-risk myelodysplastic syndromes with a possible role in disease prognosis and therapy resistance. Therefore, SBSN may be useful in diagnosing several diseases, and other roles of SBSN as a secreted protein in serum should be investigated.

## Acknowledgements

The authors would like to thank the staff at the Department of Oral and Maxillofacial Surgery for their helpful suggestions, Ms Miho Yoshihara for secretarial assistance, Dr Shintaro Ohnuma and Dr Kenji Mishima of the Division of Pathology in the Department of Oral Diagnostic Sciences for their pathological diagnostic advice, and Dr Kiyohito Sasa and Dr Ryutaro Kamijyo of Oral Biochemistry for their assistance with several experiments.

## Funding

The present study was supported by Grants-in-Aid for Scientific Research (KAKENHI) from the Japan Society for the Promotion of Science (JSPS) (Grant-in-Aid for Scientific Research C) (grant no. 22K10201) and (Grant in-Aid for Early-Career Scientists) (grant no. 20K18738).

## Availability of data and materials

The datasets used and/or analyzed during the current study are available from the corresponding author on reasonable request.

## Authors' contributions

AH significantly contributed to and performed the present study, prepared the figures, and wrote the manuscript. YM conceived the idea for the study. YA, MW, MN, SM and MK performed experiments. ToS and TaS helped draft the figures and manuscript. All the authors have read and approved the final version of the manuscript. YM and TaS confirm the authenticity of all the raw data.

## Ethics approval and consent to participate

The present study was approved (approval nos. 14033 and 14034) by the Animal Care and Use Committee of Showa University (Tokyo, Japan) and was conducted in accordance with the Showa University Animal Guidelines for Animal Experiments.

## Patient consent for publication

Not applicable.

## Competing interests

The authors declare that they have no competing interests.

## References

1. Singh P, Rai A, Verma AK, Alsahli MA, Rahmani AH, Almatroodi SA, Alrumaihi F, Dev K, Sinha A, Sankhwar S and Dohare R: Survival-based biomarker module identification associated with oral squamous cell carcinoma (OSCC). *Biology (Basel)* 10: 760, 2021.
2. Kim JW, Park Y, Roh JL, Cho KJ, Choi SH, Nam SY and Kim SY: Prognostic value of glucosylceramide synthase and P-glycoprotein expression in oral cavity cancer. *Int J Clin Oncol* 21: 883-889, 2016.
3. Sasahira T and Kirita T: Hallmarks of cancer-related newly prognostic factors of oral squamous cell carcinoma. *Int J Mol Sci* 19: 2413, 2018.
4. Jing X, Yang F, Shao C, Wei K, Xie M, Shen H and Shu Y: Role of hypoxia in cancer therapy by regulating the tumor microenvironment. *Mol Cancer* 18: 157, 2019.
5. Arnetz B: Tumor microenvironment. *Medicina (Kaunas)* 56: 15, 2019.
6. Wigerup C, Pålman S and Bexell D: Therapeutic targeting of hypoxia and hypoxia-inducible factors in cancer. *Pharmacol Ther* 164: 152-169, 2016.
7. Wilson WR and Hay MP: Targeting hypoxia in cancer therapy. *Nat Rev Cancer* 11: 393-410, 2011.
8. Lagory EL and Giaccia AJ: The ever-expanding role of HIF in tumour and stromal biology. *Nat Cell Biol* 18: 356-365, 2016.
9. Zhong H, De Marzo AM, Laughner E, Lim M, Hilton DA, Zagzag D, Buechler P, Isaacs WB, Semenza GL and Simons JW: Overexpression of hypoxia-inducible factor 1alpha in common human cancers and their metastases. *Cancer Res* 59: 5830-5835, 1999.
10. Semenza GL: Hypoxia-inducible factors: Mediators of cancer progression and targets for cancer therapy. *Trends Pharmacol Sci* 33: 207-214, 2012.
11. Park GT, Lim SE, Jang SI and Morasso MI: Suprabasin, a novel epidermal differentiation marker and potential cornified envelope precursor. *J Biol Chem* 277: 45195-45202, 2002.

12. Nakazawa S, Shimauchi T, Funakoshi A, Aoshima M, Phadungsaksawasdi P, Sakabe JI, Asakawa S, Hirasawa N, Ito T and Tokura Y: Suprabasin-null mice retain skin barrier function and show high contact hypersensitivity to nickel upon oral nickel loading. *Sci Rep* 10: 14559, 2020.
13. Glazer CA, Smith IM, Ochs MF, Begum S, Westra W, Chang SS, Sun W, Bhan S, Khan Z, Ahrendt S and Califano JA: Integrative discovery of epigenetically derepressed cancer testis antigens in NSCLC. *PLoS One* 4: e8189, 2009.
14. Formolo CA, Williams R, Gordish-Dressman H, MacDonald TJ, Lee NH and Hathout Y: Secretome signature of invasive glioblastoma multiforme. *J Proteome Res* 10: 3149-3159, 2011.
15. Alam MT, Nagao-Kitamoto H, Ohga N, Akiyama K, Maishi N, Kawamoto T, Shinohara N, Taketomi A, Shindoh M, Hida Y and Hida K: Suprabasin as a novel tumor endothelial cell marker. *Cancer Sci* 105: 1533-1540, 2014.
16. Zhu J, Wu G, Li Q, Gong H, Song J, Cao L, Wu S, Song L and Jiang L: Overexpression of suprabasin is associated with proliferation and tumorigenicity of esophageal squamous cell carcinoma. *Sci Rep* 6: 21549, 2016.
17. Shao C, Tan M, Bishop JA, Liu J, Bai W, Gaykalova DA, Ogawa T, Vikani AR, Agrawal Y, Li RJ, *et al*: Suprabasin is hypomethylated and associated with metastasis in salivary adenoid cystic carcinoma. *PLoS One* 7: e48582, 2012.
18. Takahashi K, Asano N, Imatani A, Kondo Y, Saito M, Takeuchi A, Jin X, Saito M, Hattai W, Asanuma K, *et al*: Sox2 induces tumorigenesis and angiogenesis of early-stage esophageal squamous cell carcinoma through secretion of suprabasin. *Carcinogenesis* 41: 1543-1552, 2020.
19. Liu S, Zhou X, Peng X, Li M, Ren B, Cheng G and Cheng L: *Porphyromonas gingivalis* promotes immunoevasion of oral cancer by protecting cancer from macrophage attack. *J Immunol* 205: 282-289, 2020.
20. Hubackova S, Pribyl M, Kyjácova L, Moudra A, Dzijak R, Salovska B, Strnad H, Tambor V, Imrichova T, Svec J, *et al*: Interferon-regulated suprabasin is essential for stress-induced stem-like cell conversion and therapy resistance of human malignancies. *Mol Oncol* 13: 1467-1489, 2019.
21. Kato K, Mukudai Y, Motohashi H, Ito C, Kamoshida S, Shimane T, Kondo S and Shirota T: Opposite effects of tumor protein D (TPD) 52 and TPD54 on oral squamous cell carcinoma cells. *Int J Oncol* 50: 1634-1646, 2017.
22. Abe Y, Mukudai Y, Kurihara M, Hourai A, Chikuda J, Yaso A, Kato K, Shimane T and Shirota T: Tumor protein D52 is upregulated in oral squamous carcinoma cells under hypoxia in a hypoxia-inducible-factor-independent manner and is involved in cell death resistance. *Cell Biosci* 11: 122, 2021.
23. Momose F, Araida T, Negishi A, Ichijo H, Shioda S and Sasaki S: Variant sublines with different metastatic potentials selected in nude mice from human oral squamous cell carcinomas. *J Oral Pathol Med* 18: 391-395, 1989.
24. Livak KJ and Schmittgen TD: Analysis of relative gene expression data using real-time quantitative PCR and the 2(-Delta Delta C(T)) method. *Methods* 25: 402-408, 2001.
25. Mukudai Y, Kondo S, Fujita A, Yoshihama Y, Shirota T and Shintani S: Tumor protein D54 is a negative regulator of extracellular matrix-dependent migration and attachment in oral squamous cell carcinoma-derived cell lines. *Cell Oncol (Dordr)* 36: 233-245, 2013.
26. Nakamura S, Mukudai Y, Chikuda J, Zhang M, Shigemori H, Yazawa K, Kondo S, Shimane T and Shirota T: Combinational anti-tumor effects of chemicals from *Paeonia lutea* leaf extract in oral squamous cell carcinoma cells. *Anticancer Res* 41: 6077-6086, 2021.
27. Chen Y, Lu B, Yang Q, Fearn C, Yates JR III and Lee JD: Combined integrin phosphoproteomic analyses and small interfering RNA-based functional screening identify key regulators for cancer cell adhesion and migration. *Cancer Res* 69: 3713-3720, 2009.
28. Kurihara M, Mukudai Y, Watanabe H, Asakura M, Abe Y, Hourai A, Chikuda J, Shimane T and Shirota T: Autophagy prevents osteocyte cell death under hypoxic conditions. *Cells Tissues Organs* 210: 326-338, 2021.
29. Eckert AW, Kappler M, Schubert J and Taubert H: Correlation of expression of hypoxia-related proteins with prognosis in oral squamous cell carcinoma patients. *Oral Maxillofac Surg* 16: 189-196, 2012.
30. Zhang D, Lv FL and Wang GH: Effects of HIF-1 $\alpha$  on diabetic retinopathy angiogenesis and VEGF expression. *Eur Rev Med Pharmacol Sci* 22: 5071-5076, 2018.
31. Di Nezza LA, Jobling T and Salamonsen LA: Progesterone suppresses matrix metalloproteinase production in endometrial cancer. *Gynecol Oncol* 89: 325-333, 2003.
32. Scheau C, Badarau IA, Costache R, Caruntu C, Mihai GL, Didilescu AC, Constantin C and Neagu M: The role of matrix metalloproteinases in the epithelial-mesenchymal transition of hepatocellular carcinoma. *Anal Cell Pathol (Amst)* 2019: 9423907, 2019.
33. Kim SH, Cho NH, Kim K, Lee JS, Koo BS, Kim JH, Chang JH and Choi EC: Correlations of oral tongue cancer invasion with matrix metalloproteinases (MMPs) and vascular endothelial growth factor (VEGF) expression. *J Surg Oncol* 93: 330-337, 2006.
34. González-González R, Ortiz-Sarabia G, Molina-Frechero N, Salas-Pacheco JM, Salas-Pacheco SM, Lavallo-Carrasco J, López-Verdín S, Tremillo-Maldonado O and Bologna-Molina R: Epithelial-mesenchymal transition associated with head and neck squamous cell carcinomas: A review. *Cancers (Basel)* 13: 3027, 2021.
35. Aseervatham J and Ogbureke KUE: Effects of DSPP and MMP20 silencing on adhesion, metastasis, angiogenesis, and epithelial-mesenchymal transition proteins in oral squamous cell carcinoma cells. *Int J Mol Sci* 21: 4734, 2020.
36. De Craene BD and Berx G: Regulatory networks defining EMT during cancer initiation and progression. *Nat Rev Cancer* 13: 97-110, 2013.
37. Melincovici CS, Boşca AB, Şuşman S, Mărginean M, Mihu C, Istrate M, Moldovan IM, Roman AL and Mihu CM: Vascular endothelial growth factor (VEGF)-key factor in normal and pathological angiogenesis. *Rom J Morphol Embryol* 59: 455-467, 2018.
38. Höckel M and Vaupel P: Tumor hypoxia: Definitions and current clinical, biologic, and molecular aspects. *J Natl Cancer Inst* 93: 266-276, 2001.
39. Ribeiro M, Teixeira SR, Azevedo MN, Fraga AC Jr, Gontijo APM and Vêncio EF: Expression of hypoxia-induced factor-1  $\alpha$  in early-stage and in metastatic oral squamous cell carcinoma. *Tumour Biol* 39: 1010428317695527, 2017.
40. Zimna A and Kurpisz M: Hypoxia-inducible factor-1 in physiological and pathophysiological angiogenesis: Applications and therapies. *Biomed Res Int* 2015: 549412, 2015.
41. Pribyl M, Hodny Z and Kubikova I: Suprabasin-a review. *Genes (Basel)* 12: 108, 2021.
42. Tan H, Wang L and Liu Z: Suprabasin: Role in human cancers and other diseases. *Mol Biol Rep* 49: 1453-1461, 2022.
43. Kabeya Y, Mizushima N, Ueno T, Yamamoto A, Kirisako T, Noda T, Kominami E, Ohsumi Y and Yoshimori T: LC3, a mammalian homologue of yeast Apg8p, is localized in autophagosome membranes after processing. *EMBO J* 19: 5720-5728, 2000.
44. Bjørkøy G, Lamark T, Brech A, Outzen H, Perander M, Overvatn A, Stenmark H and Johansen T: p62/SQSTM1 forms protein aggregates degraded by autophagy and has a protective effect on huntingtin-induced cell death. *J Cell Biol* 171: 603-614, 2005.
45. Yang X, Yu DD, Yan F, Jing YY, Han ZP, Sun K, Liang L, Hou J and Wei LX: The role of autophagy induced by tumor microenvironment in different cells and stages of cancer. *Cell Biosci* 5: 14, 2015.
46. Su Z, Yang Z, Xu Y, Chen Y and Yu Q: Apoptosis, autophagy, necroptosis, and cancer metastasis. *Mol Cancer* 14: 48, 2015.
47. Li X, He S and Ma B: Autophagy and autophagy-related proteins in cancer. *Mol Cancer* 19: 12, 2020.
48. Towers CG, Wodetzki D and Thorburn A: Autophagy and cancer: Modulation of cell death pathways and cancer cell adaptations. *J Cell Biol* 219: e201909033, 2020.
49. Amaravadi R, Kimmelman AC and White E: Recent insights into the function of autophagy in cancer. *Genes Dev* 30: 1913-1930, 2016.
50. Zanutelli MR, Zhang J and Reinhart-King CA: Mechanoreponsive metabolism in cancer cell migration and metastasis. *Cell Metab* 33: 1307-1321, 2021.
51. Shih CH, Ozawa S, Ando N, Ueda M and Kitajima M: Vascular endothelial growth factor expression predicts outcome and lymph node metastasis in squamous cell carcinoma of the esophagus. *Clin Cancer Res* 6: 1161-1168, 2000.
52. Aoshima M, Phadungsaksawasdi P, Nakazawa S, Iwasaki M, Sakabe JI, Umayahara T, Yatagai T, Ikeya S, Shimauchi T and Tokura Y: Decreased expression of suprabasin induces aberrant differentiation and apoptosis of epidermal keratinocytes: Possible role for atopic dermatitis. *J Dermatol Sci* 95: 107-112, 2019.
53. Pribyl M, Hubackova S, Moudra A, Vancurova M, Polackova H, Stopka T, Jonasova A, Bokorova R, Fuchs O, Stritesky J, *et al*: Aberrantly elevated suprabasin in the bone marrow as a candidate biomarker of advanced disease state in myelodysplastic syndromes. *Mol Oncol* 14: 2403-2419, 2020.

